IEICE TRANSACTIONS
on Communications

PAPER

Free-Space Optical Systems over Correlated Atmospheric Fading Channels: Spatial Diversity or Multihop Relaying?*

Phuc V. TRINH[†], *Member*, **Thanh V. PHAM**[††], *Student Member*, and **Anh T. PHAM**[††a)], *Member*

SUMMARY   Both spatial diversity and multihop relaying are considered to be effective methods for mitigating the impact of atmospheric turbulence-induced fading on the performance of free-space optical (FSO) systems. Multihop relaying can significantly reduce the impact of fading by relaying the information over a number of shorter hops. However, it is not feasible or economical to deploy relays in many practical scenarios. Spatial diversity could substantially reduce the fading variance by introducing additional degrees of freedom in the spatial domain. Nevertheless, its superiority is diminished when the fading sub-channels are correlated. In this paper, our aim is to study the fundamental performance limits of spatial diversity suffering from correlated Gamma-Gamma (G-G) fading channels in multihop coherent FSO systems. For the performance analysis, we propose to approximate the sum of correlated G-G random variables (RVs) as a G-G RV, which is then verified by the Kolmogorov-Smirnov (KS) goodness-of-fit statistical test. Performance metrics, including the outage probability and the ergodic capacity, are newly derived in closed-form expressions and thoroughly investigated. Monte-Carlo (M-C) simulations are also performed to validate the analytical results.
key words: *FSO systems, spatial diversity, relaying techniques, atmospheric turbulence, Gamma-Gamma channels, correlated fading*

1. Introduction

Free-space optical (FSO) communications, which can provide full-duplex, gigabits per second connections in a license-free spectrum, has become a promising candidate for access, metro and mobile backhaul networks [1]. One of the main challenges in FSO systems is the negative impact of atmospheric turbulence-induced fading, especially when the link range is longer than 1 km. Over the years, many techniques have been proposed to deal with this problem, including spatial diversity and multihop relaying transmission.

Multihop relaying transmission, with its ability to utilize shorter distances in the resulting hops, not only mitigates the distance-dependent turbulence strength and atmospheric loss, but also avoids the light-of-sight requirement. The performance of multihop systems with various

relaying strategies has been extensively studied for intensity modulation/direct detection (IM/DD) FSO systems [2]–[4]. Recently, coherent FSO systems, which offer a significant performance enhancement compared to their IM/DD counterparts, have received remarkable attentions thanks to recent advances in digital signal processing [5]. The adoption of multihop relaying in coherent FSO systems has been reported recently for amplify-and-forward (AF) [6], [7] and decode-and-forward (DF) [8] relaying techniques. It is obvious that the fading can be considerably mitigated by employing a large number of relays, however this is not a cost-effective solution.

On the other hand, spatial diversity provides a less complex but more economical solution, especially in the domain of FSO communications. This introduces additional degrees of freedom in the spatial domain, hence substantially reduces the fading variance. The performance of spatial diversity has been widely studied in both IM/DD and coherent FSO systems [9]–[18]. Nevertheless, the efficiency of spatial diversity is diminished when the fading among underlying sub-channels is correlated, i.e., the separation among receive apertures is smaller than the correlation length of the fading [15]–[18], for which the correlated log-normal [15], [16] and Gamma-Gamma (G-G) [17], [18] models were considered.

The goal of this paper is to study the performance limits of spatial diversity suffering from correlated fading channels in multihop coherent FSO systems. The popular G-G model is employed as it is suitable for a wide range of practical atmospheric conditions. In particular, we aim to clarify how the correlation level quantitatively limits the advantage of the spatial diversity, and to determine when the deployment of a new relay becomes necessary for a given link range and atmospheric conditions of FSO systems.

1.1 Related Studies

In most of previous studies on the performance of FSO systems with spatial diversity achieved by employing multiple transmit/receive apertures, *independent fading* channels were assumed [9]–[14]. Regarding the *correlated fading*, the performance of FSO systems with spatial diversity over G-G channels has been examined assuming a simplified model of channel correlation, e.g., the exponential correlation model [17], [18]. This model, which is borrowed from radio frequency (RF) communications, does not represent the characteristics of atmospheric turbulence channels in FSO systems. Therefore, several studies have been recently performed as

an effort to investigate the impact of channel conditions on the atmospheric turbulence-induced fading correlation [19]–[21]. In [19] and [20], by means of wave-optics and Monte-Carlo (M-C) simulations, the effects of turbulence strength, aperture diameter, aperture separation, and link range on the channel correlation have been clarified for receive diversity and transmit diversity systems, respectively. However, since simulation methods only focus on specific examples, it is difficult to extend the results to general cases. To deal with this issue, in [21], the authors have presented the correlation coefficient as a function of the above-mentioned parameters. Based on this result, an analytical study should be conducted to examine the effects of parameterized channel correlation on the performance of FSO systems. This paper therefore attempts to fill in this gap.

1.2 Main Contributions

Our key contributions in this paper are therefore threefold. *Firstly*, we analytically study the fundamental performance limits of spatial diversity under correlated G-G fading in multihop coherent FSO systems. *Secondly*, to analyze the performance of the considered system, we propose a method to accurately approximate the sum of correlated G-G random variables (RVs). Specially, the sum of correlated G-G RVs is approximated as a single G-G RV whose parameters can be obtained in simple closed-form expressions. The approximating G-G RV is then used as a benchmark to analyze the system performance. The error behaviors of the approximation for different numbers of summands and correlation coefficients are also investigated by employing the Kolmogorov-Smirnov (KS) goodness-of-fit statistical test. *Thirdly*, employing the proposed method, closed-form expressions of the outage probability and the ergodic capacity are newly derived for both DF and AF relaying schemes, considering the effects on channel correlation of the link range, the turbulence strength, the number of receive apertures and the spacing between them.

The remainder of the paper is organized as follows. In Sect. 2, the system description is presented along with the system assumptions. Section 3 presents the channel model and the correlation model. The approximation on the sum of correlated G-G RVs is introduced in Sect. 4. In Sect. 5, multihop transmission with DF and AF relaying techniques is explained. The outage probability and the ergodic capacity of the system are investigated in Sect. 6. Finally, Sect. 7 describes the numerical analysis and Sect. 8 concludes the paper.

2. System Description

We consider a full-duplex multihop FSO system in which there are $N - 1$ ($N \geq 1$) relay nodes assisting the communication between the source node and the destination node. The ith ($1 \leq i \leq N$) relay node (the destination is indexed as the Nth node) is equipped with M_i receive apertures (along with photodetectors), thereby creating N single-input multiple-
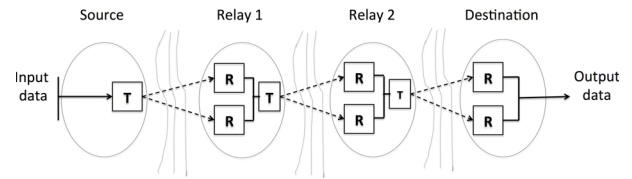
Fig. 1 Multihop SIMO system with two relay nodes and two receive apertures at each node.

output (SIMO) links. The total aperture area is assumed to be equal to that of single aperture systems in order to ensure a fair comparison. The diameter of each aperture is considered to be far smaller than the link range, resulting in the case of a point receiver, i.e., aperture averaging effect is limited. Figure 1 shows an example of the system under consideration with $N = 3$ and $M_i = 2$. Furthermore, we consider coherent (i.e., heterodyne detection) FSO systems. At the relay nodes, the incoming optical field associated with each receive aperture is coherently combined with a local oscillator (LO) field before it falls onto the photodetector. The electrical signals collected from M photodetectors are then combined using *Maximum Ratio Combining* (MRC). Thereafter, the signal is either amplified or decoded before being forwarded to the next node.

Atmospheric turbulence-induced fading is a slow time-varying process with the coherence time in the order of a few milliseconds. As a result, at typical bit-rates of FSO systems (i.e., Gigabit per second), the fading remains constant over a large number of transmitted bits. Therefore, it is feasible to assume that the receiver can perfectly estimate the fading amplitude. It is also reasonable to assume that the fading among the sub-channels in each SIMO link is identical and possibly correlated, while the fading among the SIMO links is independent but not necessarily identical (i.n.i.d).

3. Channel Model

3.1 Atmospheric Channel Attenuation

The channel attenuation is caused by both molecular absorption and aerosol scattering suspended in the air. The total channel attenuation is given as $a = \frac{A}{\pi \left(\frac{\phi L}{2} \right)^2} \exp(-\beta_\nu L)$, where $A = \pi D^2 / 4$, L, ϕ and β_ν are the area of the receive aperture (with D denotes the receiver aperture diameter), the link range, the angle of divergence of the optical beam in radian, and the atmospheric extinction coefficient, respectively [22].

3.2 G-G Turbulence-Induced Fading

The G-G model (also known as the Generalized-K model) has been widely used to characterize the turbulence-induced fading as it can cover a wide range of turbulence conditions [22]. Let X be a RV representing the turbulent fading. According to the G-G model, X is considered to be the product of two independent Gamma RVs which describe the fad-

TRINH et al.: FSO SYSTEMS OVER CORRELATED ATMOSPHERIC FADING CHANNELS: SPATIAL DIVERSITY OR MULTIHOP RELAYING?

2035

ing caused by the large-scale and the small-scale turbulence. Assuming that the average of X is normalized to unity, its probability density function (PDF) is given as

$$f_X(x) = \frac{2(\alpha\beta/\Omega)^{(\alpha+\beta)/2}}{\Gamma(\alpha)\Gamma(\beta)} x^{(\alpha+\beta)/2-1} K_{\alpha-\beta}\left(2\sqrt{\frac{\alpha\beta x}{\Omega}}\right),$$
(1)

where $\Gamma(\cdot)$ is the gamma function, $K_{\alpha-\beta}(\cdot)$ is the modified Bessel function of the second kind and order $\alpha - \beta$, and the mean $\Omega = 1$ [23]. α and β are the PDF parameters describing the turbulence with respect to the large-scale and small-scale turbulence, and in the case of zero-inner scale they are given by [23]

$$\alpha = \left\{\exp\left[\frac{0.49\sigma_R^2}{\left(1 + 1.11\sigma_R^{12/5}\right)^{7/6}}\right] - 1\right\}^{-1},$$

$$\beta = \left\{\exp\left[\frac{0.51\sigma_R^2}{\left(1 + 0.69\sigma_R^{12/5}\right)^{5/6}}\right] - 1\right\}^{-1}.$$
(2)

The parameter σ_R^2 is the Rytov variance, assuming plane wave propagation, it is given by $\sigma_R^2 = 1.23C_n^2 k^{7/6}L^{11/6}$, where $k = 2\pi/\lambda$, with λ is the optical wavelength, denotes the optical wave number, L is the link range and C_n^2 is the altitude-dependent index of the refractive structure parameter determining the turbulence strength. Typically, C_n^2 varies from 10^{-17} to 10^{-12} according to the strength of atmospheric turbulence [24]. The pth moment of X is given by $\mathbb{E}[X^p] = \frac{\Gamma(\alpha+p)\Gamma(\beta+p)}{\Gamma(\alpha)\Gamma(\beta)}(\alpha\beta/\Omega)^{-p}$ [25]. Its cumulative distribution function (CDF) is also given as

$$F_X(x) = \frac{1}{\Gamma(\alpha)\Gamma(\beta)} G_{1,3}^{2,1}\left[\frac{\alpha\beta x}{\Omega}\middle| \begin{matrix} 1 \\ \alpha, \beta, 0 \end{matrix}\right],$$
(3)

where $G_{p,q}^{m,n}[\cdot]$ is the Meijer's G-function [25].

3.3 Channel Correlation Analysis

3.3.1 General Turbulence Conditions

In practical MIMO FSO systems, the presence of correlation among sub-channels is sometimes inevitable, especially, for an extended link and/or relatively small aperture separation [15], [19], [20]. This negative effect significantly reduces the spatial diversity gain. Hence, the prediction of the channel correlation plays a key role in evaluating the overall system performance. The correlation coefficient, denoted as ρ, as a function of the turbulence strength, the link range, the aperture diameter, and the aperture separation between any two receive apertures separated by the distance d, can be given as $\rho = \frac{\zeta(d)}{\zeta(0)}$ [21]. Here, $\zeta(d)$ is the spatial covariance function defined as

$$\zeta(d) = \exp\left\{8\pi^2 k^2 L \int_0^1 \int_0^\infty \kappa\Phi_{n,\text{eff}}(\kappa)J_0(\kappa d)\right.$$
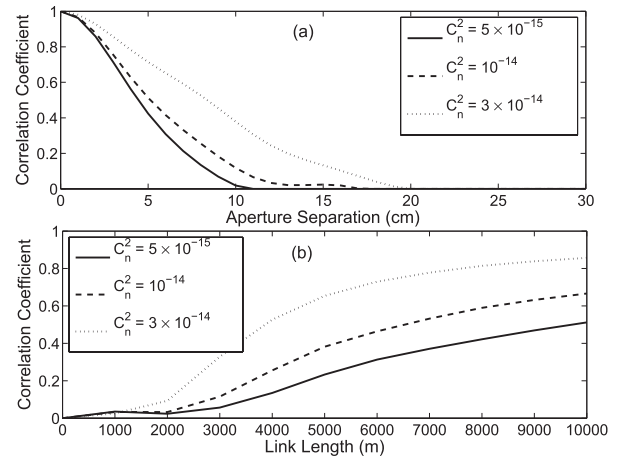
Fig. 2 (a) Correlation coefficient versus aperture separation for different values of turbulence strength and link range $L = 4000$ m; (b) Correlation coefficient versus link range for different values of turbulence strength and aperture separation $d = 8$ cm.

$$\left.\times \exp\left(\frac{-D^2\kappa^2}{16}\right)\left[1 - \cos\left(\frac{L\kappa^2\xi}{k}\right)\right] \text{d}\kappa \text{d}\xi\right\} - 1,$$
(4)

where D is the aperture diameter, $J_0(\cdot)$ is the Bessel function of the first kind and zero order, and $\Phi_{n,\text{eff}}(\kappa)$ represents the effective atmospheric spectrum. Assuming the case of zero-inner scale and infinity-outer scale, $\Phi_{n,\text{eff}}(\kappa)$ is given by [22]

$$\Phi_{n,\text{eff}}(\kappa) = 0.033C_n^2\kappa^{-11/3}\left[\exp\left(-\frac{\kappa^2}{\kappa_{X,0}^2}\right) + \frac{\kappa^{11/3}}{(\kappa^2 + \kappa_{Y,0}^2)^{11/6}}\right],$$
(5)

with $\kappa_{X,0}^2 = \frac{k}{L}\frac{2.61}{1+1.11\sigma_R^2}$, $\kappa_{Y,0}^2 = \frac{3k}{L}\left(1 + 0.69\sigma_R^{12/5}\right)$.

The relation between the correlation coefficient ρ and different system parameters is demonstrated in Fig. 2. More specifically, in Fig. 2a, it is seen that there is a *threshold value* of the aperture separation where the fading switches from correlated to independent fading. This value is referred to as the *correlation length* of the turbulence fading. When aperture separation is less than this threshold value, the correlation coefficient begins to increase rapidly. On the other hand, the turbulence strength also plays an important role in determining the correlation condition. For example, it is seen in Fig. 2b that the correlation coefficient is negligible in weak and moderate turbulence regimes, when the link range is shorter than 3000 m. The correlation coefficient is however increased quickly in the case of strong turbulence and becomes higher than 0.3.

3.3.2 G-G Turbulence Condition

To present a general model for correlated G-G subchannels, the fading correlation ρ can be considered as arising partly from large- and small-scale turbulent eddies. Originally in [26], the G-G RVs is derived from the product of two independent Gamma RVs, which represent the large- and

small-scale turbulent eddies. As a consequence for the G-G model, the fading correlation can be represented in terms of the correlation coefficients between large- and small-scale turbulence components. Given $X_i \sim \Gamma\Gamma(\alpha_i, \beta_i, \Omega_i)^\dagger$, $X_j \sim \Gamma\Gamma(\alpha_j, \beta_j, \Omega_j)$ and the independence of large- and small-scale fading, the correlation coefficient between X_i and X_j is given by [27]

$$\rho_{ij} = \rho_{ji} = \frac{\text{Cov}(X_i, X_j)}{\sqrt{\text{Var}(X_i)\text{Var}(X_j)}}$$
$$= \frac{\rho_{s_{ij}}\sqrt{\alpha_i \alpha_j} + \rho_{l_{ij}}\sqrt{\beta_i \beta_j} + \rho_{s_{ij}}\rho_{l_{ij}}}{(\sqrt{\alpha_i + \beta_i + 1})(\sqrt{\alpha_j + \beta_j + 1})}, \quad (6)$$

where $\rho_{s_{ij}}$ and $\rho_{l_{ij}}$ represent small- and large-scale fading coefficients between X_i and X_j, respectively. Cov$(\cdot)$ and Var$(\cdot)$ denote the covariance and variance operators. Specifically, for the case of identically correlated (i.e., $\rho_{s_{ij}} = \rho_s$ and $\rho_{l_{ij}} = \rho_l$) and identically distributed G-G RVs (i.e., $\alpha_i = \alpha_j = \alpha$, $\beta_i = \beta_j = \beta$ and $\Omega_i = \Omega_j = \Omega$), Eq. (6) can be re-written as the correlation coefficient ρ between two arbitrary sub-channels as follows.

$$\rho = \frac{\rho_s \alpha + \rho_l \beta + \rho_s \rho_l}{\alpha + \beta + 1}. \quad (7)$$

In general, ρ_s and ρ_l should be appropriately set to predict the system performance accurately. From Eq. (7), mathematically speaking, given a value of ρ, there is an infinite number of solutions for ρ_s and ρ_l. However, in the *strong turbulence regime*, the intensity fluctuations arising from the small-scale turbulence can be averaged out effectively, which leads to $\rho_s \approx 0$. On the other hand, under *weak-to-moderate turbulence regime*, all turbulent eddies of any size affect the propagating beam, resulting in $\rho_s = \rho_l$. Finally, under *moderate-to-strong turbulence regime*[††], both large- and small-scale turbulence components simultaneously affect the multiple apertures, while the correlation for the large-scale turbulence component is higher. Therefore, we have $\rho_s < \rho_l$ and the system performance lies between that of the cases when $\rho_s \approx 0$ and $\rho_s = \rho_l$ [19].

4. Approximation to the Sum of Correlated G-G Random Variables

4.1 Approximation Method

In this section, we investigate the distribution of the sum of correlated G-G RVs as the foundation for further performance analysis in the paper. Let $\{X_i \sim \Gamma\Gamma(\alpha_i, \beta_i, \Omega_i)\}_1^M$ be a set of M correlated G-G RVs. The sum of them is defined as

---

[†]In this paper, we use the notation $X \sim \Gamma\Gamma(\alpha, \beta, \Omega)$ for indicating that the RV X follows the G-G distribution with parameters (α, β, Ω).

[††]For the sake of simplicity, this uncertain case is excluded in our analysis.

$$Z = \sum_{i=1}^{M} X_i. \quad (8)$$

The exact statistic of Z, however, remains unknown. An approximation approach, therefore, is of great interest due to the computational advantage while still providing a good accuracy. For the case of correlated G-G RVs, several approximation methods have been proposed in the literature. In [28], the sum of two correlated G-G RVs was approximated by an α-μ RV based on the moment matching method. Numerical results confirmed a good accuracy of the approach. However, the parameters of the approximating α-μ RV can only be obtained numerically using software packages (e.g., MATLAB) due to the difficult nonlinear equations. The use of a Gamma RV as the approximating RV has been studied in [27]. The main drawback of this approach is the need of adjustment parameters, which are introduced to tighten the accuracy in the case of large values of the standard deviation of the summands. In [29], [30], the PDF and CDF of the sum of correlated G-G RVs were approximately represented through finite series forms that are cumbersome to use in analyzing the performance of our considered SIMO multihop systems.

In this study, our purpose is thus to approximate the sum of correlated G-G RVs in such a way that is simple for further usages while offering a sufficient accuracy. To do so, we propose to use a G-G RV as the approximating RV as has been studied for the case of independent G-G RVs in [31]. It is noted that the authors in [27] also mentioned the use of a G-G RV for approximation. Nevertheless, expressions for deriving the parameters of the approximating G-G RV have not been clarified.

First, let us define the following definition.

Definition [32]: The amount of fading (AF) of the RV X is defined as the ratio of the variance to the square of the mean

$$\text{AF} = \frac{\text{Var}(X)}{(\mathbb{E}(X))^2}, \quad (9)$$

where $\mathbb{E}(\cdot)$ is the expectation operator. For a RV $X \sim \Gamma\Gamma(\alpha, \beta, \Omega)$, the AF is given by

$$\text{AF} = \frac{1}{\alpha} + \frac{1}{\beta} + \frac{1}{\alpha\beta}. \quad (10)$$
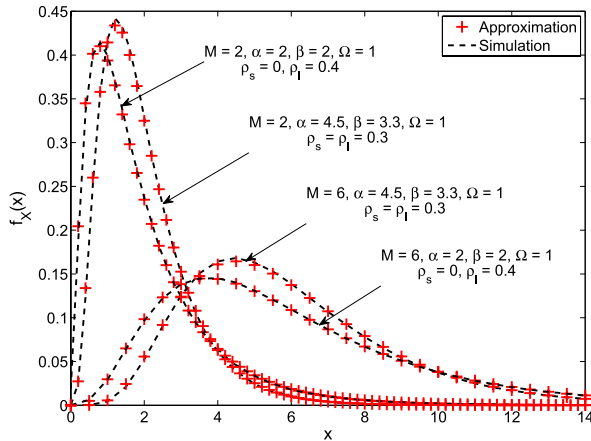
It is noted that in the context of atmospheric turbulence channels, the AF is termed as *scintillation index*, which represents the severity of the turbulence-induced fading. Assuming that Z is approximated by a G-G RV $Y \sim \Gamma\Gamma(\alpha_s, \beta_s, \Omega_s)$. Following the approach in [31], the basic idea of our approximation is to match the AF of Z with that of Y. The parameters of Y can then be obtained in closed-form expressions.

Since the fading among the sub-channels in each SIMO link can be assumed to be identical, as mentioned in Section II, we only focus on the case of identically correlated and identically distributed (i.c.i.d) G-G RVs X_i (i.e., $\alpha_i = \alpha_j = \alpha$, $\beta_i = \beta_j = \beta$, $\Omega_i = \Omega_j = \Omega$, $\rho_{s_i} = \rho_{s_j} = \rho_s$ and
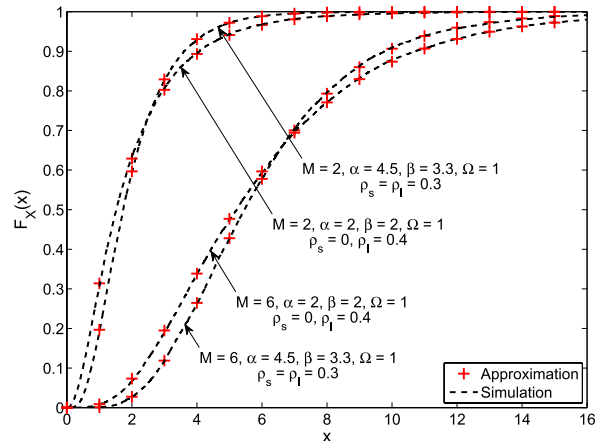
TRINH et al.: FSO SYSTEMS OVER CORRELATED ATMOSPHERIC FADING CHANNELS: SPATIAL DIVERSITY OR MULTIHOP RELAYING?

2037

Fig. 3 PDF plots for the sum of correlated G-G RVs and the approximating G-G RV.

Fig. 4 CDF plots for the sum of correlated G-G RVs and the approximating G-G RV.

$\rho_{l_i} = \rho_{l_j} = \rho_l, \forall i \neq j)^{\dagger}$. In this case, the AF for Z is expressed by [27, Eq. (14)]

$$
\begin{aligned}
\mathsf{AF}_s &= \frac{1 - \rho_s}{M\beta} + \frac{1 - \rho_l}{M\alpha} + \frac{1 - \rho_s\rho_l}{M\alpha\beta} + \frac{\rho_s}{\beta} + \frac{\rho_l}{\alpha} + \frac{\rho_s\rho_l}{\alpha\beta} \\
&= \frac{(\alpha + \beta + 1)(1 - \rho + M\rho)}{M\alpha\beta}.
\end{aligned} \tag{11}
$$

Proposition 1: The parameters α_s, β_s and Ω_s of the approximating RV Y can be given by

$$\alpha_s = t\beta_s, \tag{12}$$

$$\beta_s = \frac{(t+1) + \sqrt{(t+1)^2 + 4t\mathsf{AF}_s}}{2t\mathsf{AF}_s}, \tag{13}$$

$$\Omega_s = M\Omega, \tag{14}$$

where $t = \frac{\alpha}{\beta}$.

Proof: See Appendix A.

4.2 Numerical Examples

We demonstrate the accuracy of the proposed method by comparing the statistic of the approximating RV Y with that of the simulation data for the i.c.i.d case, which is of our interest in this paper. The simulated PDF and CDF of the sum of G-G RVs generated from 2×10^6 samples by M-C method are used for reference. The generation of M correlated G-G RVs for the simulation is based on generating two separate sets of M correlated Gamma RVs. In this study, we employ the Decomposition Method [33] to generate correlated Gamma RVs with arbitrary correlation coefficients. In Figs. 3 and 4, we compare the PDFs and CDFs of the approximating G-G RV with that of the simulation data, respectively.

---

†Similar method can be applied for the general case of arbitrarily correlated but not necessary identically distributed (a.c.n.i.d), we nevertheless do not include here due to the limitation of paper length.

Two different scenarios, $\rho_s = \rho_l$ and $\rho_s = 0$, $\rho_l > 0$, are considered. It is seen that for various values of α, β, ρ_s, ρ_l and M, there are always excellent agreements between the approximation and simulation results. To quantitatively evaluate the error behavior of the proposed approximation, we employ the Kolmogorov-Smirnov (KS) goodness-of-fit statistical test, which measures the maximum value T of the absolute difference between the empirical CDF of the sum Z and the analytical CDF of the approximating RV Y, i.e.,

$$T \overset{\Delta}{=} \left| F_Z(x) - F_Y(x) \right|. \tag{15}$$

To verify an approximation, the KS goodness-of-fit test compares the statistical test value T with a critical level T_{max} for a given significance level ϕ. An approximation is said to be accepted with significance level $(1-\phi)$ if $T < T_{max}$, while it is considered to be rejected with the same significance level if $T > T_{max}$. The critical value of T_{max} is given by $T_{max} = \sqrt{-\frac{1}{2v} \ln \frac{\phi}{2}}$, where ϕ is the significance level and v is the number of samples of RV for the simulation. Here, we choose the typical values $\phi = 5\%$ and $v = 10^4$, resulting in $T_{max} = 0.0136$ [34].

Figure 5 presents the KS-statistical test T of our proposed approximation method with $M = 2$, $\rho = 0.4$ ($\rho_s = \rho_l$), $\Omega_1 = \Omega_2 = 1$ for different values of α and β. The result is obtained by averaging the results of 50 simulation runs. We observed that the proposed method is valid (i.e., $T \leq 0.0136$) when $\alpha \geq 2$ and $\beta \geq 2$. On the other hand, the test is not satisfied when either $\alpha < 2$ or $\beta < 2$, which generally corresponds to the strong turbulence regime. The proposed method however still offers a reasonable accuracy (i.e., the analytical results still agree well with the simulation ones) to a certain performance level of interest even in strong turbulence regime and $M = 2$ as shown later in Sect. 7 (Figs. 7–10 and 12). As for larger M, we present an additional KS-statistical test in Fig. 6 for $M = 6$, $\rho = 0.6$ ($\rho_s = \rho_l$), $\Omega_1 = \Omega_2 = 1$. In this case, the test is accepted for any values of α and β that are larger than or equal to 1. This agrees with the observation in [31] that the larger M results
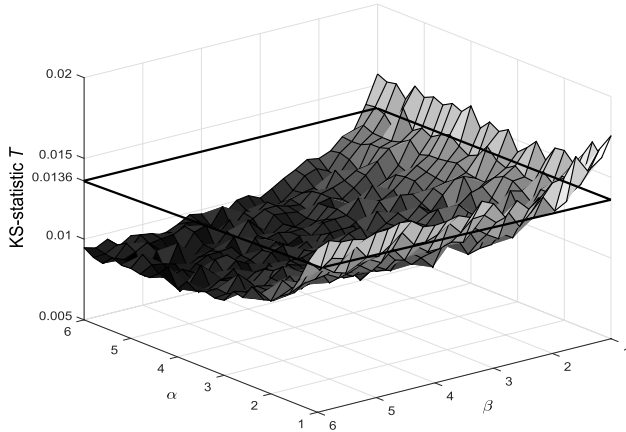
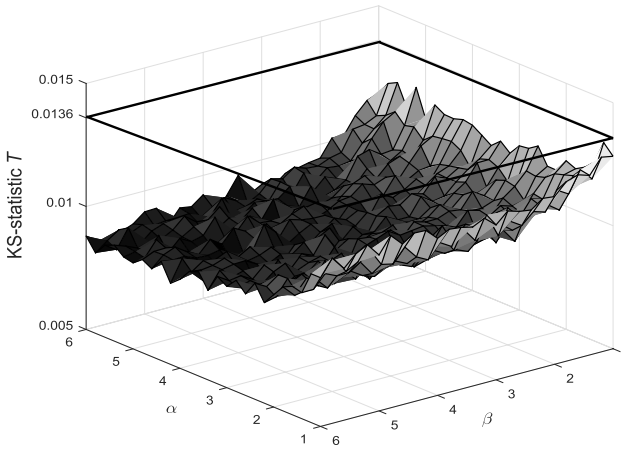**Fig. 5** KS goodness-of-fit test for $M = 2$ and $\rho = 0.4$.

Fig. 6 KS goodness-of-fit test for $M = 6$ and $\rho = 0.6$.

in the better accuracy of the approximation.

5. Multihop Transmission

In this section, we analyze the multihop transmission of the proposed FSO system utilizing DF and AF relaying techniques. For the sake of simplicity, from now on, we assume that the number of receive apertures at each hop is chosen to be equal, i.e., $M_i = M$ ($1 \le i \le N$).

5.1 DF Relaying

In DF relaying, the relay node decodes the received signal, then remodulates and retransmits it to the next node. We assume that all receivers' parameters are the same and the total average transmitted power, denoted as P_t, is allocated equally to each transmit aperture. The ith receiver has a LO power of $w_i^2 P_{LO}$, where $\sum_{m=1}^{M} w_{i,m}^2 = 1$ so that the total power of N local oscillators is the same with that of a single aperture receiver (P_{LO}) to ensure a fair comparison. In addition, we assume that the phase noise can be fully compensated at the receiver by means of a phase-locked loop [35]. After heterodyning, combining Rthe multiple received

signals from M receive apertures, and lowpass filtering, the output signal at the ith relay node ($i = 1, 2, ..., N$) can be given as

$$y_i(t) = \sum_{m=1}^{M} x_{i,m}(t) + \sum_{m=1}^{M} n_{i,m}(t), \qquad (16)$$

where $x_{i,m}(t)$ and $n_{i,m}(t)$ are the information carrying part representing the AC terms and the noise term at the mth receive aperture of the ith hop. Each noise term $n_{i,m}(t)$ is dominated by the LO shot noise which can be modeled as an AWGN with zero mean and variance of $\sigma_{i,m}^2 = 2q w_{i,m}^2 R P_{LO} \Delta f$ [36], where q, R and Δf respectively denote the electron charge, receiver's responsivity, and effective noise bandwidth. Hence, the total noise variance can be given as $\sigma_i^2 = 2q R P_{LO} \Delta f$. Using the result from [35], $x_{i,m}(t)$ can be written as

$$x_{i,m}(t) = 2R \sqrt{P_{i,m} w_{i,m}^2 P_{LO}} \cos(2\pi f_{IF} t + \phi_m), \quad (17)$$

where $f_{IF} = f_c - f_{LO}$ is the intermediate frequency with f_c and f_{LO} are the carrier frequency and LO frequency, respectively. The received optical power at the mth receive aperture of the ith hop can be expressed as $P_{i,m} = \frac{a_i P_t X_{i,m}}{M_i N}$, where P_t is the total transmitted power, $a_i = a(L_i)/a(L)$ denotes the normalized channel attenuation at the ith hop, and $X_{i,m}$ is the turbulence-induced fading associated with the mth aperture.

The signal-to-noise ratio (SNR) of an optical receiver is defined as the ratio of the time-averaged AC photocurrent power and the total noise variance [36]. Thus, the instantaneous SNR at the ith hop can be given as

$$\gamma_i = \frac{\langle x_{i,m}^2(t) \rangle}{\sigma_i^2} = \frac{2R^2 \left(\sum_{m=1}^{M} w_{i,m} \sqrt{P_{i,m}} \right)^2 P_{LO}}{\sigma_i^2}$$

$$= \frac{R \left(\sum_{m=1}^{M} w_{i,m} \sqrt{P_{i,m}} \right)^2}{q \Delta f}. \qquad (18)$$

By means of MRC, $w_{i,m}$ ($1 \le m \le M$) is chosen so that the SNR is maximized. By using the Cauchy-Schwartz inequality, the maximum SNR can be given as

$$\gamma_i = \frac{R}{q \Delta f} \sum_{m=1}^{M} P_{i,m} = \frac{a_i \gamma_0}{MN} \sum_{m=1}^{M} X_{i,m}, \qquad (19)$$

where $\gamma_0 = RP_t/q\Delta f$ is the total path loss-free and turbulence-free SNR of the system. It is assumed that $X_{i,m}$ ($m = 1, 2, ..., M$) are identically distributed and statistically correlated G-G RVs with parameters ($\alpha_{i,0}, \beta_{i,0}, 1$) and the correlation coefficient between $X_{i,m}$ and $X_{i,p}$ is ρ_{mp}. According to the previous section, $\sum_{m=1}^{M} X_{i,m}$ can be well approximated by a RV $X_i \sim \Gamma\Gamma(\alpha_i, \beta_i, M)$, where α_i and β_i are obtained following the procedures in the *Proposition 1*. The instantaneous SNR at the ith node can be approximated by

TRINH et al.: FSO SYSTEMS OVER CORRELATED ATMOSPHERIC FADING CHANNELS: SPATIAL DIVERSITY OR MULTIHOP RELAYING?

2039

$$\gamma_i = \frac{a_i \gamma_0}{MN} X_i. \tag{20}$$

After a simple transformation of random variable, the distribution of γ_i can be expressed as

$$f_{\gamma_i}(\gamma) = \frac{2(N\alpha_i\beta_i/a_i\gamma_0)^{(\alpha_i+\beta_i)/2}}{\Gamma(\alpha_i)\Gamma(\beta_i)} \gamma^{(\alpha_i+\beta_i)/2-1}$$

$$\times K_{\alpha_i-\beta_i}\left(2\sqrt{\frac{N\alpha_i\beta_i\gamma}{a_i\gamma_0}}\right). \tag{21}$$

5.2 AF Relaying

Using the proposed approximation, the received signal at the first relay can be rewritten as

$$y_1 = 2R\sqrt{P_1 P_{LO}} \cos(\omega_{IF}t + \phi_m) + n_1(t), \tag{22}$$

where $P_1 = a_1 X_1 P_t/MN$. The signal y_1 is amplified by the gain G_1 so that it is normalized to unity. The amplified electrical signal is then used to drive an external modulator to modulate the carrier optical signal. The obtained optical signal is then transmitted to the second node. The received signal at the second node can be given as

$$y_2 = (2R)^2 G_1 \sqrt{P_1 P_2 P_{LO}^2} \cos^2(\omega_{IF}t + \phi_m)$$

$$+ 2RG_1\sqrt{P_2 P_{LO}} \cos(\omega_{IF}t + \phi_m)n_1(t) + n_2(t), \tag{23}$$

where $P_2 = a_2 X_2 P_t/MN$. The signal y_2 is amplified by G_2, optically modulated and transmitted to the next node. The received signal at the third node can be given as

$$y_3 = (2R)^3 G_1 G_2 \sqrt{P_1 P_2 P_3 P_{LO}^3} \cos^3(\omega_{IF}t + \phi_m)$$

$$+ (2R)^2 G_1 G_2 \sqrt{P_2 P_3 P_{LO}^2} \cos^2(\omega_{IF}t + \phi_m)n_1(t)$$

$$+ 2RG_2\sqrt{P_3 P_{LO}} \cos(\omega_{IF}t + \phi_m)n_2(t) + n_3(t), \tag{24}$$

where $P_3 = a_3 X_3 P_t/MN$. Repeating the above procedures, eventually, the received signal at the destination node can be expressed as

$$y_N = (2R)^N \left(\prod_{i=1}^{N-1} G_i\right) \sqrt{\prod_{i=1}^{N}(P_i P_{LO})} \cos^N(\omega_{IF}t + \phi_m)$$

$$+ \sum_{i=1}^{N-1} (2R)^{N-i} \left(\prod_{j=i}^{N-1} G_j\right) \sqrt{\prod_{j=i+1}^{N}(P_j P_{LO})}$$

$$\times \cos^{N-i}(\omega_{IF}t + \phi_m) + n_N(t), \tag{25}$$

where $P_i = a_i X_i P_t/MN$. The inverse end-to-end SNR is thus given by

$$\frac{1}{\gamma_{end}} = \frac{\left(\sum_{i=1}^{N-1}\sigma_i^2 \prod_{j=i+1}^{N}\left(2R^2 P_j P_{LO}\right)\prod_{j=i}^{N-1} G_j^2 + \sigma_N^2\right)}{\prod_{i=1}^{N}\left(2R^2 P_i P_{LO}\right)\prod_{i=1}^{N-1} G_i^2}. \tag{26}$$

With the assumption of available CSIs at receivers, the relay node is able to perform a variable-gain amplification. More specifically, each relay has an access to the instantaneous CSI of its previous hop. Therefore, to satisfy the average power constraint at the output of the ith relay, based on Eq. (26), the gain G_i can be given as $G_i^2 = \frac{1}{2R^2 P_i P_{LO} + \sigma_i^2}$. Using this gain, the end-to-end SNR can be calculated as

$$\gamma_{end} = \left(\prod_{i=1}^{N}\left(1 + \frac{1}{\gamma_i}\right) - 1\right)^{-1}, \tag{27}$$

where $\gamma_i = \left(2R^2 P_i P_{LO}\right)/\sigma_i^2$, which is identical to Eq. (20).

6. Performance Analysis

6.1 Ergodic Channel Capacity Analysis

It is well known that the atmospheric turbulence over FSO channels is slow in fading, which is equivalent to communication over channels where there is a nonzero probability that any given transmission rate cannot be supported by the channel. Since the coherence time of the channel is in the order of milliseconds, atmospheric turbulence-induced fading remains constant over a large number of transmitted bits [9], [37]. Without any delay constraints, if the codeword extends over at least several atmospheric coherence times, which allows coding across both deep and shallow fade channel realizations, the fast fading regime can be assumed. With proper coding and interleaving, the capacity can be expressed as an average over many independent fades of the atmospheric channel. The average (i.e., ergodic) capacity is the expectation with respect to the gains of the instantaneous capacity [38]. Since there is no interference issue with full-duplex transmission for an FSO communication relaying system, the capacity of the full-duplex transmission is simply double than that of the half-duplex transmission. In this section, closed-form expressions of the ergodic channel capacity are derived for both DF and AF relaying schemes.

6.1.1 DF Relaying

The capacity of a fading channel depends on what is known about the CSI at the transmitter and the receiver. Under the condition that the CSI is only available at the receiving side, power or rate adaptation techniques cannot be realized at the transmitter. The overall system achievable rate is therefore the minimum of the achievable rates over each hop [39]. Let C_i ($i = 1, ..., N$) be the capacity of the ith link, then the ergodic capacity in DF multihop system can be expressed as $C = \min\{C_1, C_2, ..., C_N\}$. The capacity of the ith SIMO full-duplex link for an average power constraint P_t/N can be calculated as $C_i = \frac{2}{N}\int_0^\infty B\log_2(1 + \gamma_i) f_{\gamma_i}(\gamma_i)d\gamma_i$, where B denotes the transmission bandwidth and γ_i is given in Eq. (20). A closed-form expression for C_i can be given in terms of the Meijer-G function as

$$C_i = \frac{2B}{N\ln(2)} \frac{(N\alpha_i\beta_i/a_i\gamma_0)^{(\alpha_i+\beta_i)/2}}{\Gamma(\alpha_i)\Gamma(\beta_i)}$$
$$\times G_{2,4}^{4,1}\left[\frac{N\alpha_i\beta_i}{a_i\gamma_0}\middle| \begin{array}{c} -\frac{\alpha_i+\beta_i}{2}, \ 1-\frac{\alpha_i+\beta_i}{2} \\ \frac{\alpha_i-\beta_i}{2}, \ \frac{-\alpha_i+\beta_i}{2}, \ -\frac{\alpha_i+\beta_i}{2}, \ -\frac{\alpha_i+\beta_i}{2} \end{array}\right]. \quad (28)$$

Proof of Eq. (28) can be found in Appendix B.

6.1.2 AF Relaying

For full-duplex AF relaying systems, the ergodic capacity is a function of the end-to-end SNR and it is given as $C = \frac{2}{N}\mathbb{E}(\log_2(1+\gamma_{\text{end}}))$. The end-to-end SNR given in Eq. (27) is difficult to extract in a tractable form. Therefore, the framework for computing the ergodic capacity of multihop variable-gain relay system presented in [40] is very useful. According to this framework, the ergodic capacity is calculated as

$$C = \frac{2}{N\ln(2)}\sum_{q=1}^{Q}\frac{1}{q}\left(\prod_{i=1}^{N}\mathbb{E}\left(\left(1+\frac{1}{\gamma_i}\right)^{-q}\right)\right) + R_Q, \quad (29)$$

where $Q \geq 1$ and R_Q is a truncation error. In this paper, in order to obtain accurate results, Q is set to be 15000. A closed-form expression for $\mathbb{E}\left((1+1/\gamma_i)^{-q}\right)$ can be given in terms of the Meijer-G function as

$$\mathbb{E}\left(\left(1+\frac{1}{\gamma_i}\right)^{-q}\right) = \frac{(N\alpha_i\beta_i/a_i\gamma_0)^{(\alpha_i+\beta_i)/2}}{\Gamma(\alpha_i)\Gamma(\beta_i)\Gamma(q)}$$
$$\times G_{3,1}^{1,3}\left[\frac{a_i\gamma_0}{N\alpha_i\beta_i}\middle| \begin{array}{c} 1+\frac{\alpha_i+\beta_i}{2}, \ 1-\frac{\alpha_i-\beta_i}{2}, \ 1+\frac{\alpha_i-\beta_i}{2} \\ q+\frac{\alpha_i+\beta_i}{2} \end{array}\right]. \quad (30)$$

Proof of Eq. (30) can be found in Appendix C.

6.2 Outage Probability Analysis

In addition to the ergodic capacity, which is an important performance measure, the outage probability is another meaningful performance metric that should be investigated. Due to the slowly time-varying nature of optical fade in FSO communication channels, there is a non-zero probability that any given transmission rate cannot be supported by the channel. Consequently, the outage probability is defined as the probability that the transmission rate exceeds the instantaneous capacity of the channel. The outage probability at a given rate R_0 is given as $P_{\text{out}}(R_0) = \text{Prob}(C(\text{SNR}) < R_0)$ [41]. Since $C(\cdot)$ monotonically increases with respect to the SNR, $P_{\text{out}}(R_0) = \text{Prob}(\text{SNR} < \gamma_{\text{th}})$, where γ_{th} is the SNR threshold.

6.2.1 DF Relaying

The outage probability of the ith intermediate SIMO link can be given as $P_{out,SIMO,i} = \text{Prob}(\gamma_i < \gamma_{\text{th}})$. Substituting γ_i from Eq. (20), we obtain

$$P_{out,SIMO,i} = \text{Prob}\left(X_i < \frac{M_iN\gamma_{\text{th}}}{a_i\gamma_0}\right) = F_{X_i}\left(\frac{M_iN\gamma_{\text{th}}}{a_i\gamma_0}\right), \quad (31)$$

where $F_{X_i}(\cdot)$ is given as in Eq. (3). In multihop DF relaying systems, an outage occurs when any of the intermediate SIMO links fails. The outage probability is thus given by

$$P_{out,DF} = 1 - \prod_{i=1}^{N}\left(1-P_{out,SIMO,i}\right)$$
$$= 1 - \prod_{i=1}^{N}1 - \frac{G_{1,3}^{2,1}\left[\frac{N\alpha_i\beta_i\gamma_{\text{th}}}{a_i\gamma_0}\middle| \begin{array}{c} 1 \\ \alpha_i, \beta_i, 0 \end{array}\right]}{\Gamma(\alpha_i)\Gamma(\beta_i)}. \quad (32)$$

6.2.2 AF Relaying

For AF relaying, no decoding process is performed at relaying nodes, hence the outage probability will depend on the end-to-end SNR at the destination node. The distribution of the end-to-end SNR in Eq. (27) is difficult to obtain. However, Eq. (27) can be tightly approximated by $\gamma_{\text{end}} \approx \left(\sum_{i=1}^{N}\frac{1}{\gamma_i}\right)^{-1}$ [42]. This refers to the ideal case of AF relaying where equivalently the gain is adjusted with respect to the channel state, aiming to compensate signal attenuation caused by the channel attenuation and turbulent fading, i.e., $G_i = \frac{M}{(a_iX_i)}$. In other words, the relay just amplifies the incoming signal with the inverse of the channel intensity gain of the previous hop, regardless of the noise of that hop).

Numerical Evaluation: To evaluate the exact outage performance, $P_{out,AF}$ can be numerically evaluated as

$$P_{out,AF} \approx \text{Prob}\left(\gamma_{end} < \gamma_{\text{th}}\right) = \text{Prob}\left(\frac{1}{\gamma_{end}} > \frac{1}{\gamma_{\text{th}}}\right)$$
$$= 1 - F_Y\left(\frac{a_i\gamma_0}{MN\gamma_{\text{th}}}\right), \quad (33)$$

where Y is a random variable defined as $Y = \sum_{i=1}^{N}1/X_i$ and $F_Y(\cdot)$ denotes the CDF of Y. $F_Y(\cdot)$ can be calculated in terms of the inverse Laplace transform as in $F_Y(y) = \mathscr{L}_s^{-1}\left\{\frac{M_Y(s)}{s}\right\}(y)$, where $M_Y(s) = \int_0^\infty \exp(-sy)f_Y(y)\mathrm{d}y$ is the moment generating function (MGF) of Y [43]. If $M_Y(s)$ is given in a closed-form expression, Eq. (33) can be numerically evaluated using inverse Laplace transform function supported in standard mathematical softwares (e.g., MATLAB). Noting that the fading among N point-to-point SIMO links is independent, $M_Y(s)$ can be given as

$$M_Y(s) = \prod_{i=1}^{N}M_{1/X_i}(s). \quad (34)$$

$M_{1/X_i}(s)$ can be calculated as

$$M_{1/X_i}(s) = \frac{(\alpha_i\beta_i/M)^{(\alpha_i+\beta_i)/2}}{\Gamma(\alpha_i)\Gamma(\beta_i)} \times s^{(\alpha_i+\beta_i)/2}$$

TRINH et al.: FSO SYSTEMS OVER CORRELATED ATMOSPHERIC FADING CHANNELS: SPATIAL DIVERSITY OR MULTIHOP RELAYING?

2041

$$\times G_{0,3}^{3,0} \left[\frac{\alpha_i \beta_i s}{M} \middle| \frac{\alpha_i - \beta_i}{2}, \frac{-\alpha_i + \beta_i}{2}, -\frac{\alpha_i + \beta_i}{2} \right].$$

(35)

Proof of Eq. (35) can be found in Appendix D. Substituting Eq. (35) and Eq. (34) in Eq. (33), we obtain the exact-form expression for the outage probability in the case of AF relaying.

Closed-form Expression of Lower Bound: It is worthy to note that the equivalent SNR in Eq. (27) is not tractable in a closed-form expression due to the difficulty in deriving its statistics. Therefore, an upper bound for the end-to-end SNR γ_{end} can be derived by utilizing the inequality between harmonic and geometric means for $\gamma_1, \gamma_2, \cdots, \gamma_N$, which is given as in [44]

$$\gamma_{\text{end}} \le \gamma_{\text{b}} = \frac{1}{N} \prod_{i=1}^{N} \gamma_i^{1/N}.$$

(36)

For CSI-assisted relays, a lower bound of the outage probability can be obtained in a closed-form expression as

$$P_{out,AF} = \frac{G_{3N,N}^{N,2N} \left[\frac{\prod_{i=1}^{N} \frac{a_i}{\alpha_i \beta_i}}{N^{2N}} \left(\frac{\gamma_0}{\gamma_{th}} \right)^N \middle| \begin{matrix} \Xi_N, \Delta(N,1) \\ \Delta(N,0) \end{matrix} \right]}{\prod_{i=1}^{N} \Gamma(\alpha_i) \Gamma(\beta_i)},$$

(37)

where $\Xi_N = \{1 - \beta_1, 1 - \alpha_1, \cdots, 1 - \beta_N, 1 - \alpha_N\}$, and $\Delta(k,l) = \left\{ \frac{l}{k}, \frac{l+1}{k}, \cdots, \frac{l+k-1}{k} \right\}$. Details of the derivation of Eq. (37) can be found in Appendix E.

## 7. Numerical Results and Discussions

In this section, unless otherwise noted, system parameters under consideration are selected as specified below. The optical wavelength of $\lambda = 1.55\,\mu m$ is chosen. The AWGN noise variance $N_0 = 2 \times 10^{-14}$ is assumed for all receiver noises. The atmospheric extinction coefficient $\beta_v = 0.1$ dB/km, the angle of divergence of the optical beam $\theta = 10^{-3}$ radian. For the sake of a fair comparison, the total aperture area of the multiple apertures system is chosen to be equal to that of a single aperture system, with the aperture diameter of 8 cm. Furthermore, we assume an equal distance between any two consecutive relay nodes.

7.1 Independent Fading

First, let us consider the outage performance in the case of independent fading where the M apertures are placed sufficiently far apart. Under a strong turbulence condition with $C_n^2 = 10^{-14}$, the outage probability of the DF relaying system as a function of the normalized SNR is shown in Fig. 7 for different numbers of hops N and receive apertures M. It is seen that, in the case of independent fading, spatial diversity is strongly preferable to the use of new relays. For instance, at a target probability of 10^{-6}, the performance of a two receive apertures ($M = 2$) system with no relay ($N = 1$) is about 10 dB better than that of a single aperture system
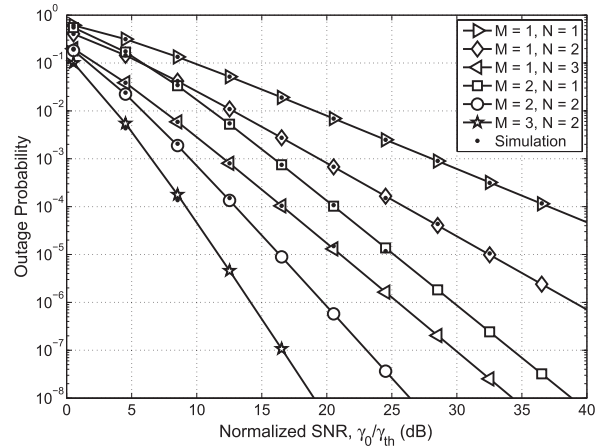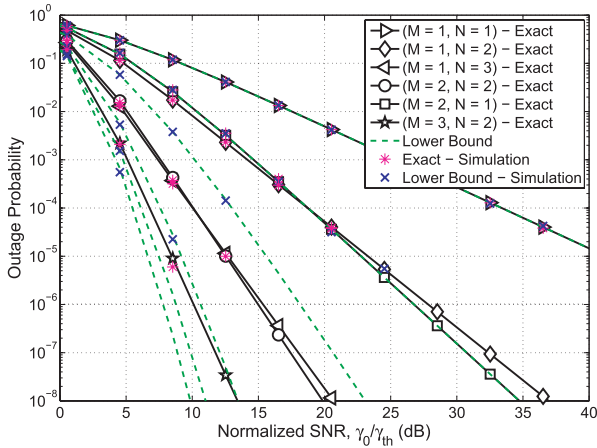

Fig. 7 DF relaying: Outage probability versus normalized SNR for independent fading with different numbers of hops and receive apertures, $C_n^2 = 10^{-14}$, $L = 8000$ m.
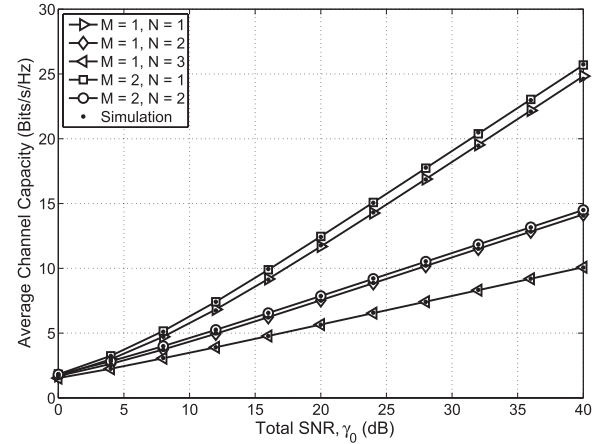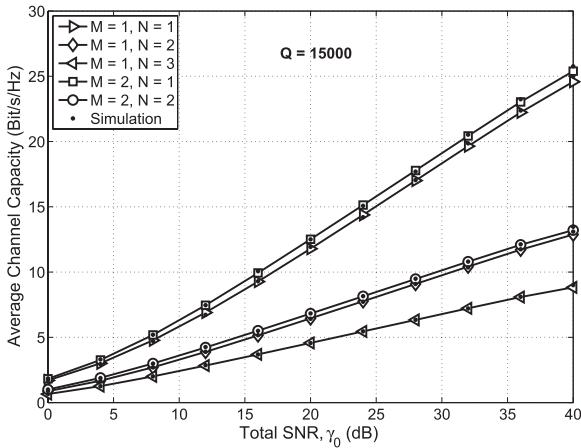

Fig. 8 DF relaying: Average channel capacity versus total SNR for independent fading with different numbers of hops and receive apertures, $C_n^2 = 10^{-14}$, $L = 8000$ m.

with one relay ($N = 2$). In another example, the ($M = 2$, $N = 2$) system outperforms the ($M = 1$, $N = 3$) with 5 dB gain. Keeping the same system settings, the ergodic capacity is shown in Fig. 8. The advantage of spatial diversity is confirmed due to the fact that the ergodic capacity is further reduced with the increase in the number of relays. In particular, it is seen in Fig. 8 that the system with $M = 1$ and $N = 3$ has the lowest capacity while the system with $M = 2$ and $N = 1$ has the highest capacity.

In Fig. 9 and Fig. 10, the outage probability and the ergodic capacity of the system operating in the AF mode are presented, however, under a weaker turbulence strength with $C_n^2 = 5 \times 10^{-15}$. Besides the exact outage probability in Fig. 9, the lower bounds are also plotted. It is noted that for the case of $N = 1$, the exact and the lower bound of the outage are the same since equality holds in the inequality in Eq. (36). It is seen that, similar to the DF case, employing spatial diversity is still preferable, especially in the case of ergodic capacity. Nevertheless, its advantage in the outage performance is not

Fig. 9 AF relaying: Outage probability versus normalized SNR for independent fading with different numbers of hops and receive apertures, $C_n^2 = 5 \times 10^{-15}$, $L = 8000$ m.

Fig. 11 DF relaying: Outage probability versus normalized SNR with different values of correlation coefficient and $N = M = 2$, $C_n^2 = 10^{-14}$, $L = 8000$ m.
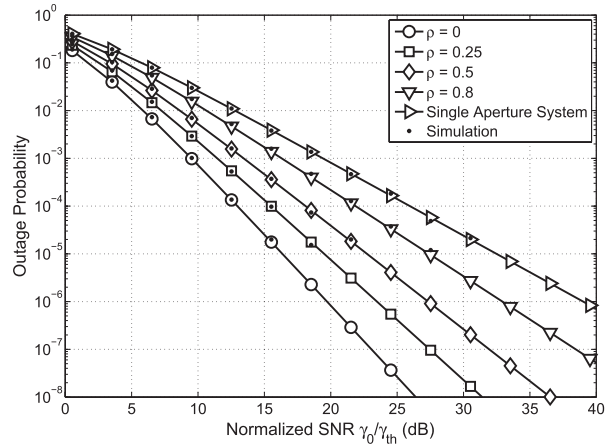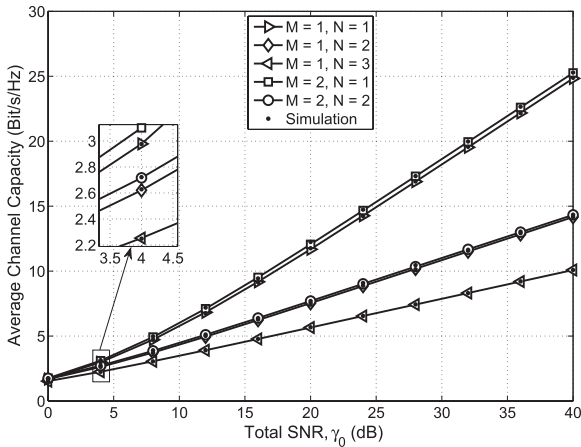

Fig. 10 AF relaying: Average channel capacity versus total SNR for independent fading with different numbers of hops and receive apertures, $C_n^2 = 5 \times 10^{-15}$, $L = 8000$ m.

the channel capacity should be carefully considered.

7.2 Correlated Fading

The previous section shows that the use of spatial diversity is effective in the case of independent fading. Nevertheless, fading independence is not always available in practice. In this section, given the correlated fading condition, we investigate the limits of employing spatial diversity in the context of multihop systems. For the sake of conciseness, only DF relaying systems are presented.

Figure 11 shows the impact of channel correlation on the outage probability of the ($M = 2, N = 2$) system. The outage probability is plotted as a function of the normalized SNR for different levels of channel correlation. The M-C simulation is also shown, and a good accuracy is observed. The negative effect of channel correlation on the system performance is clearly seen. For instance, when the correlation coefficient $\rho = 0.25$ and $\rho = 0.5$, the power penalty is around 5 dB and 11 dB at the outage probability of 10^{-6}, respectively. As the correlation increases, the outage performance comes closer to that of a single aperture system.

By comparing Fig. 11 and Fig. 7, the impact of correlated fading on the system performance can be evaluated. Specifically, when we compare ($M = 2, N = 2$) and ($M = 1, N = 3$) systems in the case of independent fading, the spatial diversity gain is about 5 dB (Fig. 7). Nevertheless, when channel correlation is considered, the gain is reduced. In particular, when the correlation coefficient $\rho = 0.25$, the penalty caused by correlation is 3 dB (as can be seen in Fig. 11 with a note that ($M = 1, N = 3$) system does not suffer from the impact of correlation). In this case, spatial diversity is still preferable as the combined gain is 2 dB. However, when the correlation coefficient is relatively high (e.g. $\rho = 0.5$), the penalty is 7.5 dB (Fig. 11) which results in a combined loss of 2.5 dB when comparing ($M = 2, N = 2$) with ($M = 1, N = 3$) system. Therefore, to guarantee the outage performance, one may consider to add more aperture,

as clear as in the case of stronger turbulence. For instance, it is seen in Fig. 9 that the outage performance of the ($M = 1$, $N = 3$) system is closer to that of ($M = 2$, $N = 2$) system in comparison with its counterparts in Fig. 7. This is due to the fact that as the turbulence strength is weaker, the fading reduction benefited from spatial diversity becomes less substantial.

Important Remarks:

- In the case of independent fading, instead of deploying many relays within a fixed link range, one may consider the utilization of fewer relays with receive diversity at each relay, which is a more cost-effective solution to achieve a targeted performance.
- The effectiveness of spatial diversity is less significant in weaker turbulence. In this case, increasing the number of relays is the better choice to further improve the system performance. Higher number of relays however has a negative impact on the ergodic capacity. Therefore, a trade-off between the outage performance and

TRINH et al.: FSO SYSTEMS OVER CORRELATED ATMOSPHERIC FADING CHANNELS: SPATIAL DIVERSITY OR MULTIHOP RELAYING?

2043

Fig. 12 DF relaying: Average channel capacity versus total SNR for correlated fading $\rho = 0.5$ with different numbers of hops and receive apertures, $C_n^2 = 10^{-14}$, $L = 8000\,\text{m}$.

e.g. to use ($M = 3$, $N = 2$) system, or to add a new relay.

In Fig. 12, the impact of channel correlation on the ergodic capacity is presented. Obviously, the correlation does have a negative impact, and in the case of strong correlation, there is no more advantage to use spatial diversity. Nevertheless, the capacity reduction caused by the increase in the number of relays still dominates. As we can see, the capacity of the ($M = 2$, $N = 1$) system is far higher than that of ($M = 1$, $N = 3$) one.

Important Remarks:

- When the correlation coefficient is small (less than 0.5), the performance gain benefited from spatial diversity in Section VII.A will remain. The spatial diversity is preferable and system design could be based on the numerical results of independent fading case.
- When the correlation coefficient is higher than 0.5, it is necessary to carefully examine the correlation penalty to determine the necessary number of apertures and relays.

8. Conclusions

This paper studied the performance limits of spatial diversity in multihop AF and DF relaying FSO systems in the presence of correlated G-G fading channels. The system performance in terms of outage probability and ergodic capacity was analytically derived in closed-form expressions. M-C simulations were used to validate the analytical results and excellent agreement between the analytical and simulation results was confirmed. Our numerical results show that the spatial diversity along with multihop transmission provides a significant performance improvement when there is no correlation or the correlation coefficient is smaller than 0.5 in fading channels. However, if the correlation coefficient is larger than 0.5 due to long link ranges and strong turbulence conditions, the advantage of spatial diversity is substantially diminished. In this case, it is necessary to carefully exam-

ine the correlation penalty to determine the combination of spatial diversity and multihop technique.

References

[1] Z. Ghassemlooy, W. Popoola, and S. Rajbhandari, Optical Wireless Comunication: System and Channel Modelling with MATLAB, CRC Press, 2012.

[2] M. Safari and M. Uysal, "Relay-assisted free-space optical communication," IEEE Trans. Wireless Commun., vol.7, no.12, pp.5441–5449, Dec. 2008.

[3] C.K. Datsikas, K. Peppas, N. Sagias, and G. Tombras, "Serial free-space optical relaying communications over Gamma-Gamma atmospheric turbulence channels," IEEE/OSA J. Opt. Commun. Netw., vol.2, no.8, pp.576–586, Aug. 2010.

[4] E. Zedini and M.-S. Alouini, "Multihop relaying over IM/DD FSO systems with pointing errors," IEEE/OSA J. Lightw. Technol., vol.33, no.23, pp.5007–5015, Dec. 2015.

[5] G. Li, "Recent advances in coherent optical communication," Adv. Opt. Photon., vol.1, no.2, pp.279–307, April 2009.

[6] J. Park, E. Lee, C. Chae, and G. Yoon, "Outage probability analysis of coherent FSO amplify-and-forward relaying systems," IEEE Photon. Technol. Lett., vol.27, no.11, pp.1204–1207, June 2015.

[7] E. Zedini and M.-S. Alouini, "On the performance of multihop heterodyne FSO systems with pointing errors," IEEE Photon. J., vol.7, no.2, Article no.790110, April 2015.

[8] S. Aghajanzadeh and M. Uysal, "Multi-hop coherent free-space optical communications over atmospheric turbulence channels," IEEE Trans. Commun., vol.59, no.6, pp.1657–1663, June 2011.

[9] E.J. Lee and V.W. S. Chan, "Part 1: Optical communication over the clear turbulent atmospheric channel using diversity," IEEE J. Sel. Areas Commun., vol.22, no.9, pp.1896–1906, Nov. 2004.

[10] S.G. Wilson, M. Brandt-Pearce, Q. Cao, and M. Baedke, "Optical repetition MIMO transmission with multipulse PPM," IEEE J. Sel. Areas Commun., vol.23, no.9, pp.1901–1910, Sept. 2005.

[11] T.A. Tsiftsis, H.G. Sandalidis, G.K. Karagiannidis, and M. Uysal, "Optical wireless links with spatial diversity over strong atmospheric turbulence channels," IEEE Trans. Wireless Commun., vol.8, no.2, pp.951–957, Feb. 2009.

[12] S.M. Aghajanzadeh and M. Uysal, "Diversity multiplexing tradeoff in coherent free-space optical systems with multiple receivers," IEEE/OSA J. Opt. Commun. Netw., vol.2, no.12, pp.1087–1094, Dec. 2010.

[13] J. Park, E. Lee, C. Chae, and G. Yoon, "Performance analysis of coherent free-space optical systems with multiple receivers," IEEE Photon. Technol. Lett., vol.27, no.9, pp.1010–1013, May 2015.

[14] C. Abou-Rjeily and A. Abdo, "Serial relaying over Gamma-Gamma MIMO FSO links: Diversity order and aperture allocation," IEEE Commun. Lett., vol.19, no.4, pp.553–556, April 2015.

[15] X. Zhu and J. Kahn, "Maximum-likelihood spatial-diversity reception on correlated turbulent free-space optical channels," Proc. IEEE Global Communications Conference (GLOBECOM), pp.1237–1241, 2000.

[16] S.M. Navidpour, M. Uysal, and M. Kavehrad, "BER performance of free-space optical transmission with spatial diversity," IEEE Trans. Wireless Commun., vol.6, no.8, pp.2813–2819, Aug. 2007.

[17] S.M. Navidpour, M. Uysal, and J. Li, "Analysis of coded wireless optical communications under correlated Gamma-Gamma channels," Proc. IEEE 60th Vehicular Technology Conference (VTC2004-Fall), pp.827–831, Sept. 2004.

[18] K.P. Peppas, G.C. Alexandropoulos, C.K. Datsikas, and F.I. Lazarakis, "Multivariate gamma-gamma distribution with exponential correlation and its applications in radio frequency and optical wireless communications," IET Microw. Antennas Propag., vol.5, no.3, pp.364–371, Feb. 2011.

[19] G. Yang, M. Khalighi, Z. Ghassemlooy, and S. Bourennane, "Per-

formance evaluation of receive-diversity free-space optical communications over correlated Gamma-Gamma fading channels," Appl. Opt., vol.52, no.24, pp.5903–5911, Aug. 2013.

[20] J.A. Anguita, M.A. Neifeld, and B.V. Vasic, "Spatial correlation and irradiance statistics in a multiple-beam terrestrial free-space optical communication link," Appl. Opt., vol.46, pp.6561–6571, Sept. 2007.

[21] Z. Chen, S. Yu, T. Wang, G. Wu, S. Wang, and W. Gu, "Channel correlation in aperture receiver diversity systems for free-space optical communication," J. Opt., vol.14, no.12, p.125710, 2012.

[22] L.C. Andrews and R.L. Phillips, Laser Beam Propagation through Random Media, 2nd ed., SPIE, Bellingham, WA, 2005.

[23] M.A. Al-Habash, R.L. Phillips, and L.C. Andrews, "Mathematical model for the irradiance probability density function of a laser beam propagating through turbulent media," Opt. Eng., vol.40, no.8, pp.1554–1562, Aug. 2001.

[24] J. Goodman, Statistical Optics, John Wiley, 1985.

[25] P.S. Bithas, N.C. Sagias, P.T. Mathiopoulos, G.K. Karagiannidis, and A.A. Rontogiannis, "On the performance analysis of digital communications over generalized-K fading channels," IEEE Commun. Lett., vol.10, no.5, pp.353–355, May 2006.

[26] M.A. Al Habash, L.C. Andrews, and R.L. Phillips, "Mathematical model for the irradiance probability density function of a laser beam propagating through turbulent media," Opt. Eng., vol.40, no.8, pp.1554–1562, 2001.

[27] S. Al-Ahmadi and H. Yanikomeroglu, "On the statistics of the sum of correlated generalized-K RVs," Proc. IEEE International Conference on Communications (ICC), pp.1–5, 2010.

[28] G. Yang, M. Khalighi, S. Bourennane, and Z. Ghassemlooy, "Approximation to the sum of two correlated Gamma-Gamma variates and its applications in free-space optical communications," IEEE Trans. Wireless Commun. Lett., vol.1, no.6, pp.621–624, 2012.

[29] G. Yang, M. Khalighi, Z. Ghassemlooy, and S. Bourennane, "Performance analysis of space-diversity free-space optical systems over the correlated Gamma-Gamma fading channel using Padé approximation method," IET Commun., vol.8, no.13, pp.2246–2255, 2014.

[30] J. Zhang, M. Matthaiou, G. Karagiannidis, and L. Dai, "On the multivariate Gamma-Gamma (Γ − Γ) distribution with arbitrary correlation and applications in wireless communications," IEEE Trans. Veh. Technol., vol.65, no.5, pp.3834–3840, DOI: 10.1109/TVT.2015.2438192, 2015.

[31] S. Al-Ahmadi and H. Yanikomeroglu, "On the approximation of the PDF of the sum of independent generalized-K RVs by another generalized-K PDF with applications to distributed antenna systems," Proc. IEEE Wireless Communications and Networking Conference, pp.1–6, 2010.

[32] A. Charash, "A study of multipath reception with unknown delays," PhD dissertation, University of California, Berkeley, CA, 1974.

[33] K. Zhang, Z. Song, and Y.L. Guan, "Simulation of Nakagami fading channels with arbitrary cross-correlation and fading parameters," IEEE Trans. Wireless Commun., vol.3, no.5, pp.1463–1468, 2004.

[34] A. Papoulis, Probability, random Variables, and stochastic processes, 3rd ed., McGraw-Hill, 1991.

[35] M. Niu, J. Cheng, and J.F. Holzman, "Error rate analysis of M-ary coherent free-space optical communication systems with K-distributed turbulence," IEEE Trans. Commun., vol.59, no.3, pp.664–668, March 2011.

[36] G.P. Agrawal, Fiber-Optical Communication Systems, Wiley, 2002.

[37] M.I. Petkovic, A.M. Cvetkovic, G.T. Djordjevic, and G.K. Karagiannidis, "Partial relay selection with outdated channel state estimation in mixed RF/FSO systems," IEEE/OSA J. Lightw. Technol., vol.33, no.13, pp.2860–2867, March 2015.

[38] A. Belmonte and J.M. Kahn, "Capacity of coherent free-space optical links using atmospheric compensation techniques," OSA Opt. Express, vol.17, no.4, pp.2763–2773, Feb. 2009.

[39] G. Farhadi and N. Beaulieu, "On the ergodic capacity of multi-hop wireless relaying systems," IEEE Trans. Wireless Commun., vol.8, no.5, pp.2286–2291, May 2009.

[40] O. Waqar, D.C. McLernon, and M. Ghogho, "Exact evaluation of ergodic capacity for multihop variable-gain relay networks: A unified framework for generalized fading channels," IEEE Trans. Veh. Technol., vol.59, no.8, pp.4181–4187, Oct. 2010.

[41] E. Biglieri, J. Proakis, and S. Shamai, "Fading channels: Information-theoretic and communications aspects," IEEE Trans. Inf. Theory, vol.44, no.6, pp.2619–2692, Oct. 1998.

[42] M.O. Hasna and M.-S. Alouini, "End-to-end performance of transmission systems with relays over Rayleigh-fading channels," IEEE Trans. Wireless Commun., vol.2, no.6, pp.1126–1131, Nov. 2003.

[43] Y.-C. Ko, M.-S. Alouini, and M.K. Simon, "Outage probability of diversity systems over generalized fading channels," IEEE Trans. Comm., vol.48, no.11, pp.1783–1787, Nov. 2000.

[44] G.K. Karagiannidis, "Performance bounds of multihop wireless communications with blind relays over generalized fading channels," IEEE Trans. Wireless Commun., vol.5, no.3, pp.498–503, March 2006.

[45] A.P. Prudnikov, Y.A. Brychkov, and O.I. Marichev, Integrals and Series. vol.3: More Special Functions, Gordon and Breach Science Publishers, 1990.

[46] A.P. Prudnikov, Y.A. Brychkov, and O.I. Marichev, Integrals and Series. vol.5: Inverse Laplace Transforms, Gordon and Breach Science Publishers, 1992.

Appendix A: Proof of Proposition 1

Firstly, Ω_s can be obtained directly by matching the first moments between Y and $\sum_{i=1}^{M} X_i$ as $\Omega_s = \sum_{i=1}^{M} \Omega_i = M\Omega$. The AF for the approximating RV Y is given by

$$\mathsf{AF} = \frac{1}{\alpha_s} + \frac{1}{\beta_s} + \frac{1}{\alpha_s \beta_s}. \tag{A·1}$$

Matching the AF of Y with that of the sum given in the Eq. (11), i.e.,

$$\frac{1}{\alpha_s} + \frac{1}{\beta_s} + \frac{1}{\alpha_s \beta_s} = \mathsf{AF}_s. \tag{A·2}$$

Since we only have the above equation, to derive α_s and β_s, it is necessary to match a higher moment (e.g., the third moment) to get one more equation. It, however, leads to complicated expressions. To avoid matching higher moment, one possible way is to assume that $\alpha_s = t\beta_s$ for some value of t which depends on the parameters of each summand of the sum. With this assumption, the Eq. (A· 2) reduces to

$$\frac{(t+1)\beta_s + 1}{t\beta_s^2} = \mathsf{AF}_s. \tag{A·3}$$

Now, the parameters α_s and β_s can be easily derived by solving a quadratic equation. An important question is how to select an appropriate value of t. For the case of i.c.i.d G-G RVs, using the same argument in [31] that is $t = \frac{\alpha}{\beta}$, the parameters α_s, β_s are given as in the Proposition 1.

Appendix B: Derivation of Eq. (28)

Substituting Eq. (21) in Eq. (28), then expressing the logarithm and the Bessel functions in terms of the Meijer-G

TRINH et al.: FSO SYSTEMS OVER CORRELATED ATMOSPHERIC FADING CHANNELS: SPATIAL DIVERSITY OR MULTIHOP RELAYING?

2045

function [45, Eq. (8.4.6.5)], [45, Eq. (8.4.23.1)], Eq. (28) can be rewritten as

$$
\begin{aligned}
C_i = {} & \frac{B}{N\ln(2)} \frac{\left(\frac{N\alpha_i\beta_i}{a_i\gamma_0}\right)^{(\alpha_i+\beta_i)/2}}{\Gamma(\alpha_i)\Gamma(\beta_i)} \int_0^\infty \gamma_i^{(\alpha_i+\beta_i)/2-1} \\
& \times G_{2,2}^{1,2}\left[\gamma_i \,\middle|\, \begin{matrix} 1, 1 \\ 1, 0 \end{matrix}\right] G_{0,2}^{2,0}\left[\frac{N\alpha_i\beta_i\gamma_i}{a_i\gamma_0} \,\middle|\, \begin{matrix} \\ \frac{\alpha_i-\beta_i}{2}, \frac{\beta_i-\alpha_i}{2} \end{matrix}\right] d\gamma_i.
\end{aligned}
\tag{A·4}
$$

Using [45, Eq. (2.24.1.1)], the integral in Eq. (A·4) can be solved, yielding Eq. (28).

Appendix C: Derivation of Eq. (30)

Following the footsteps of [40], we first have

$$
\mathbb{E}\left(\left(1+\frac{1}{\gamma_i}\right)^{-q}\right) = \int_0^\infty y^{-2}(y+1)^{-q} f_{\gamma_i}(1/y)\,dy.
\tag{A·5}
$$

Substituting Eq. (21) in Eq. (30), then expressing the Bessel functions in terms of the Meijer's G-function [45, Eq. (8.4.6.5)], the integral in Eq. (A·5) can be solved with the help of [45, Eq. (2.24.2.4)], yielding Eq. (30).

Appendix D: Derivation of Eq. (35)

From the PDF of X_i and by expressing the exponential and Bessel functions in terms of the Meijer-G functions [45, Eq. (8.4.3.1)], [45, Eq. (8.4.6.5)], we then have

$$
\begin{aligned}
\mathcal{M}_{1/X_i}(s) = {} & \int_0^\infty \exp(-s/x) f_{X_i}(x)\,dx \\
= {} & \frac{(\alpha_i\beta_i/M)^{(\alpha_i+\beta_i)/2}}{\Gamma(\alpha_i)\Gamma(\beta_i)} \int_0^\infty x^{(\alpha_i+\beta_i)/2-1} \\
& \times G_{0,1}^{1,0}\left[\frac{s}{x} \,\middle|\, \begin{matrix} \\ 0 \end{matrix}\right] G_{0,2}^{2,0}\left[\frac{\alpha_i\beta_i x}{M} \,\middle|\, \begin{matrix} \\ \frac{\alpha_i-\beta_i}{2}, \frac{\beta_i-\alpha_i}{2} \end{matrix}\right] dx.
\end{aligned}
\tag{A·6}
$$

Using [45, Eq. (8.2.2.14) and Eq. (2.24.1.1)], the integral in Eq. (A·6) can be solved, resulting in Eq. (35).

Appendix E: Derivation of Eq. (37)

Theorem 1 1: The moment generating function (MGF) of the random variable γ_b in Eq. (36) can be given as

$$
\mathcal{M}_{\gamma_b}(s) = \frac{\sqrt{N} G_{2N,N}^{N,2N}\left[\frac{1}{N^{3N}} \prod_{i=1}^{N} \frac{a_i}{\alpha_i\beta_i} (\gamma_0 s)^N \,\middle|\, \begin{matrix} \Xi_N \\ \Delta(N,0) \end{matrix}\right]}{(2\pi)^{\frac{N-1}{2}} \prod_{i=1}^{N} \Gamma(\alpha_i)\Gamma(\beta_i)},
\tag{A·7}
$$

where Ξ_N and $\Delta(N,0)$ are defined in Eq. (37).

Proof: The MGF of γ_b is defined as the Laplace transform of γ_b, which can be expressed as

$$
\mathcal{M}_{\gamma_b}(s) = \int_0^\infty \exp(-s\gamma_b) f_{\gamma_b}(\gamma)\,d\gamma.
\tag{A·8}
$$

From Eq. (36), the MGF can be expressed by means of the following N-fold integral

$$
\begin{aligned}
\mathcal{M}_{\gamma_b}(s) = {} & \int_0^\infty \cdots \int_0^\infty \exp\left(-\frac{s}{N} \prod_{i=1}^{N} \gamma_i^{\frac{1}{N}}\right) \\
& \times \prod_{i=1}^{N} f_{\gamma_i}(\gamma_i)\,d\gamma_1\cdots d\gamma_N.
\end{aligned}
\tag{A·9}
$$

With the help of [45, Eq. (8.4.3.1), Eq. (8.4.23.1)] and Eq. (21), the first integral in Eq. (A·9), denoted as J_1, i.e., the one on γ_1, can be written as

$$
\begin{aligned}
J_1 = {} & \frac{\left(\frac{N\alpha_1\beta_1}{a_1\gamma_0}\right)^{\frac{\alpha_1+\beta_1}{2}}}{\Gamma(\alpha_1)\Gamma(\beta_1)} \int_0^\infty \gamma_1^{\frac{\alpha_1+\beta_1}{2}-1} G_{0,1}^{1,0}\left[\frac{s}{N} W_2 \gamma_1^{\frac{1}{N}} \,\middle|\, \begin{matrix} \\ 0 \end{matrix}\right] \\
& \times G_{0,2}^{2,0}\left[\frac{N\alpha_1\beta_1}{a_1\gamma_0} \gamma_1 \,\middle|\, \begin{matrix} \\ \frac{\alpha_1-\beta_i}{2}, \frac{\beta_i-\alpha_i}{2} \end{matrix}\right] d\gamma_1,
\end{aligned}
\tag{A·10}
$$

where $W_i = \gamma_i^{1/N} \gamma_{i+1}^{1/N} \cdots \gamma_N^{1/N}$. Using [45, Eq. (2.24.1.1)] to solve J_1, Eq. (A·10) can be rewritten as

$$
J_1 = \frac{\sqrt{N} G_{2,N}^{N,2}\left[\frac{1}{N^{1+2N}} \left(\frac{a_1}{\alpha_1\beta_1}\right) \gamma_0 (sW_2)^N \,\middle|\, \begin{matrix} \Xi_1 \\ \Delta(N,0) \end{matrix}\right]}{(2\pi)^{\frac{N-1}{2}} \Gamma(\alpha_1)\Gamma(\beta_1)},
\tag{A·11}
$$

where $\Xi_1 = \{1-\beta_1, 1-\alpha_1\}$. By applying the similar approach, the integration on γ_2 can be written as

$$
J_2 = \frac{\sqrt{N} G_{4,N}^{N,4}\left[\frac{1}{N^{1+2N}} \prod_{i=1}^{2} \frac{a_i}{\alpha_i\beta_i} \gamma_0^2 (sW_3)^N \,\middle|\, \begin{matrix} \Xi_2 \\ \Delta(N,0) \end{matrix}\right]}{(2\pi)^{\frac{N-1}{2}} \prod_{i=1}^{2} \Gamma(\alpha_i)\Gamma(\beta_i)},
\tag{A·12}
$$

where $\Xi_2 = \{1-\beta_1, 1-\alpha_1, 1-\beta_2, 1-\alpha_2\}$. Following the same procedure, the N-fold integral in Eq. (A·9) can be expressed in a closed-form expression as in Theorem 1.

Corollary 1 1: Using Theorem 1, the cumulative distribution function (CDF) of γ_b in Eq. (36) can be given as

$$
F_{\gamma_b}(\gamma) = \frac{G_{3N,N}^{N,2N}\left[\frac{1}{N^{2N}} \prod_{i=1}^{2N} \frac{a_i}{\alpha_i\beta_i} \left(\frac{\gamma_0}{\gamma}\right)^N \,\middle|\, \begin{matrix} \Xi_N \\ \Delta(N,0) \end{matrix}\right]}{\prod_{i=1}^{N} \Gamma(\alpha_i)\Gamma(\beta_i)}.
\tag{A·13}
$$

Proof: The CDF of γ_b in Eq. (36) is defined as $F_{\gamma_b}(\gamma) = \mathcal{L}^{-1}\left[\frac{1}{s}\mathcal{M}_{\Gamma_{T_i}}(s)\right]$, where $\mathcal{L}^{-1}$ denotes the inverse Laplace transform operator. With the help of Theorem 1 and using the identity [46, Eq. (3.38.1)], a closed-form expression of $F_{\gamma_b}(\gamma)$ is obtained as in Corollary 1.

Phuc V. Trinh received the B.E. degree in electronics and telecommunications from the Posts and Telecommunications Institute of Technology (PTIT), Hanoi, Vietnam, in 2013, and the M.Sc. and Ph.D. degrees in computer science and engineering from The University of Aizu (UoA), Aizuwakamatsu, Japan, in 2015 and 2017, respectively. His study in Japan was fully funded by a Japanese government scholarship (MonbuKagaku-sho). He is currently a Researcher with the Space Communications Laboratory, National Institute of Information and Communications Technology (NICT), Tokyo, Japan. His current research interests are in the area of optical wireless communications, including modulation techniques, coding, channel modeling and simulation, and performance analysis. He is a Member of the IEEE and IEICE.

Thanh V. Pham received the B.E. and M.E. degrees in computer network systems from The University of Aizu, Japan, in 2014 and 2016, respectively, where he is currently pursuing the Ph.D. degree. His study in Japan was funded by the Japanese Government Scholarship (MonbuKagakusho). His research interests are in the area of free space optics, relay networks, and visible light communications. He is a Student Member of the IEICE.

Anh T. Pham received the B.E. and M.E. degrees in electronics engineering from the Hanoi University of Technology, Vietnam, in 1997 and 2000, respectively, and the Ph.D. degree in information and mathematical sciences from Saitama University, Japan, in 2005. From 1998 to 2002, he was with NTT Corporation, Vietnam. Since 2005, he has been a Faculty Member with The University of Aizu, where he is currently a Professor and the Head of the Computer Communications Laboratory, Division of Computer Engineering. His research interests are in the broad areas of communication theory and networking with a particular emphasis on modeling, design, and performance evaluation of wired/wireless communication systems and networks. He has authored/co-authored over 160 peer-reviewed papers on these topics. Dr. Pham is senior member of IEEE. He is also member of IEICE and OSA.